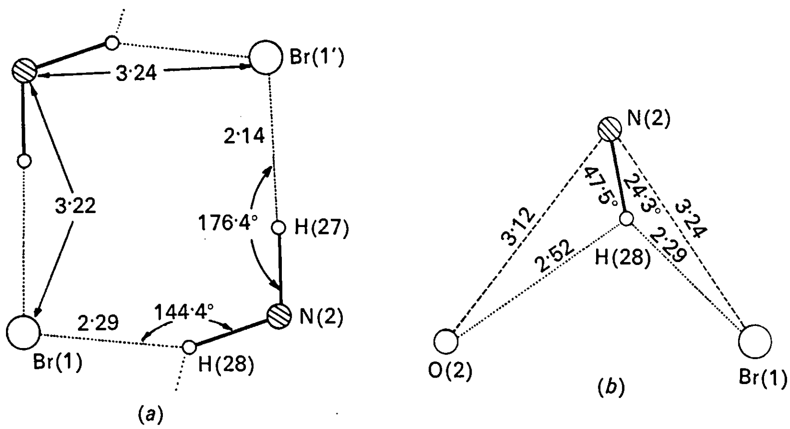

Fig. 5. The geometry of the hydrogen bonds to the amine nitrogen (distances in Å). (*a*) The ring constituted by symmetry related amine groups and bromine atoms. Projection along the *b* axis. (*b*) The bifurcated hydrogen bond, shown in the plane of the four atoms.

is in the plane and on the line Br(1′)–N(2). H(28), on the other hand, is 0·40 Å from the plane and the angle N(2)–H(28)–Br(1) is 144·4°. This makes possible weak intramolecular hydrogen bonding between N(2) and O(2) (3·12 Å) involving H(28). Conditions are favourable for a bifurcation of the H(28) bond to both O(2) and Br(1) as all involved atoms N(2), H(28), O(2) and Br(1) are in one plane. The maximum deviation is 0·02 Å for H(28). The geometry within this plane is shown in Fig. 5(*b*). It seems likely that also two weaker hydrogen bonds exist in the structure, one from O(1) to C(8) (3·11 Å) *via* H(81) and one from O(2) to C(8) (3·33 Å) via H(82).

I am greatly indebted to Prof. Sixten Abrahamsson for continuous advice and support, and to Mrs Anita Johansson for technical assistance. I also want to thank Prof. Finn Sandberg and his co-workers for crystal samples. Financial support has been obtained from the Swedish Natural Science and Swedish Medical Research Councils and the U.S. Public Health Service (GM 11653).

References

Abrahamsson, S., Aleby, S., Larsson, K., Nilsson, B., Selin, K. & Westerdahl, A. (1965). *Acta Chem. Scand.* **19**, 758.
Ahmed, F. R. & Cruickshank, D. W. J. (1953). *Acta Cryst.* **6**, 385.
Camerman, A., Camerman, N. & Trotter, J. (1965). *Acta Cryst.* **19**, 314.
Darlow, S. F. (1960). *Acta Cryst.* **13**, 683.
International Tables for X-ray Crystallography (1962). Vol. III, p. 202. Birmingham: Kynoch Press.
Michel, K.H., Sandberg, F., Haglid, F. & Norin, T. (1967). *Acta Pharm. Suec.* **4**, 97.
Przybylska, M. (1965). *Acta Cryst.* **18**, 536.
Rogers, D. & Wilson, A. J. C. (1953). *Acta Cryst.* **6**, 439.
Sandberg, F., Svanquist, L., Ödberg, M. & Sonmark, L. (1960). *Svensk Farm. Tidskr.* **64**, 541.

Acta Cryst. (1968). B**24**, 258

Nine New Zinc Sulphide Polytypes of the Family 24*L*-72*R*

By S. Mardix and O. Brafman

Department of Physics, The Hebrew University, Jerusalem, Israel

(*Received* 16 *May* 1967)

Nine hitherto unknown ZnS polytypes of the family 24*L*–72*R* were found in one crystal. Their unit-cell and Zhdanov symbols are: 24*L*(15 9); 24*L*(9 5 6 4); 24*L*(16 4 2 2); 24*L*(7 10 5 2); 24*L*(8 9 4 3); 24*L*(3 3 2 4 2 2 5 3); 24*L*(3 3 4 2 2 4 3 3); and 72*R*(6 11 5 2)$_3$; 72*R*(9 5 4 6)$_3$.

Polytypes of the 24*L*–72*R* family are already known (Farkas-Jahnke, 1965; Mardix, Brafman & Steinberger, 1967) but only one detailed structure was published, namely 24*L* (7 5 5 7) (Mardix, Brafman & Steinberger, 1967). The vapour-phase grown zinc-sulphide crystal 220/58 contained polytypic regions, nine of which were identified as new polytypes of the family 24*L*–72*R*. A microphotograph of the specimen 220/58, indicating the polytypic regions is given in Fig. 1. Table 1 gives the structures of these regions.

Table 1. *Polytype regions of specimen* 220/58 (*Fig.* 1) *and their Zhdanov symbols*

Region	Unit cell	Zhdanov symbol
a	24*L*	(15 9)
b	24*L*	(8 9 4 3)
c	72*R*	$(9\ 5\ 4\ 6)_3$
d	72*R*	$(6\ 11\ 5\ 2)_3$
e	24*L*	(7 10 5 2)
f	24*L*	(16 4 2 2)
g	24*L*	(3 3 4 2 2 4 3 3)
h	24*L*	(3 3 2 4 2 2 5 3)
i	24*L*	(9 5 6 4)

X-ray oscillation photographs about the *c* axis of the crystal were taken; Cu *K* radiation was used with a collimator of diameter 0·1 mm. Photographs of the (10.*l*) column are given in Figs. 2 to 10.

The identification of the structures was carried on by a procedure given in detail in a previously published paper (Mardix, Alexander, Brafman & Steinberger, 1967); the observed intensity order of the (10.*l*) spots is compared with the calculated intensity orders of the possible Zhdanov sequences of the same family. In each case there was only one fitting sequence; calculated intensities for this sequence are given along with the observed ones in Tables 2–10.

Table 2. *Comparison of observed and calculated intensities for the polytype* 24*L* (15 9)

l	Calc.	Obs.	*l*	Calc.	Obs.	Further observed relations between intensities
0	0	*a*				
1	466	*w*	$\bar{1}$	466	*w*	$8>7\sim 9$
2	308	*vw*	$\bar{2}$	308	*vw*	$4>1$
3	111	*vvw*	$\bar{3}$	111	*vvw*	$\bar{4}>\bar{1}$
4	1053	*w*	$\bar{4}$	1053	*w*	$2>5$
5	249	*vw*	$\bar{5}$	249	*vw*	$\bar{2}>\bar{5}$
6	1806	*s*	$\bar{6}$	1806	*s*	
7	11950	*vs*	$\bar{7}$	11950	*vs*	
8	19456	*vs*	$\bar{8}$	54045	*vvs*	
9	12430	*vs*	$\bar{9}$	12430	*vs*	
10	1980	*s*	$\overline{10}$	1980	*s*	
11	298	*vw*	$\overline{11}$	298	*vw*	
12	1452	*w*	$\overline{12}$	1452	*w*	

Table 3. *Comparison of observed and calculated intensities for the polytype* 24*L* (8 9 4 3)

l	Calc.	Obs.	*l*	Calc.	Obs.	Further observed relations between intensities
0	0	*a*				
1	548	*vw*	$\bar{1}$	883	*w*	$\bar{8}>9$
2	925	*w*	$\bar{2}$	0	*a*	$8>7$
3	1227	*w*	$\bar{3}$	295	*vw*	$6>12>5$
4	0	*a*	$\bar{4}$	3159	*s*	$\bar{7}\sim\bar{6}>\bar{4}$
5	2754	*s*	$\bar{5}$	1708	*w*	$\bar{9}\sim\overline{10}>\overline{12}$
6	5419	*s*	$\bar{6}$	5419	*s*	
7	14000	*vs*	$\bar{7}$	5438	*s*	
8	15133	*vs*	$\bar{8}$	34590	*vvs*	
9	23482	*vvs*	$\bar{9}$	5645	*s*	
10	0	*a*	$\overline{10}$	5941	*s*	
11	790	*w*	$\overline{11}$	2037	*w*	
12	4356	*s*	$\overline{12}$	4356	*s*	

Table 4. *Comparison of observed and calculated intensities for the polytype* 72*R* $(9\ 5\ 4\ 6)_3$

l	Calc.	Obs.	*l*	Calc.	Obs.	Further observed relations between intensities
1	295	*vw*	$\bar{2}$	246	*vw*	$\overline{23}>\overline{29}$
4	1583	*s*	$\bar{5}$	498	*w*	$25>19>28$
7	171	*vw*	$\bar{8}$	71	*vvw*	$\overline{20}>\overline{17}$
10	160	*vw*	$\overline{11}$	1213	*s*	$4>\overline{11}$
13	628	*w*	$\overline{14}$	1961	*s*	$13>\bar{5}$
16	756	*w*	$\overline{17}$	2777	*vs*	$1>\bar{2}>7\sim 10$
19	15260	*vvs*	$\overline{20}$	6690	*vs*	
22	2245	*vs*	$\overline{23}$	25940	*vvs*	
25	16300	*vvs*	$\overline{26}$	9502	*vs*	
28	13034	*vvs*	$\overline{29}$	11490	*vvs*	
31	801	*w*	$\overline{32}$	2064	*s*	
34	2670	*vs*	$\overline{35}$	373	*vw*	
37	327	*vw*	$\overline{38}$	2047	*s*	

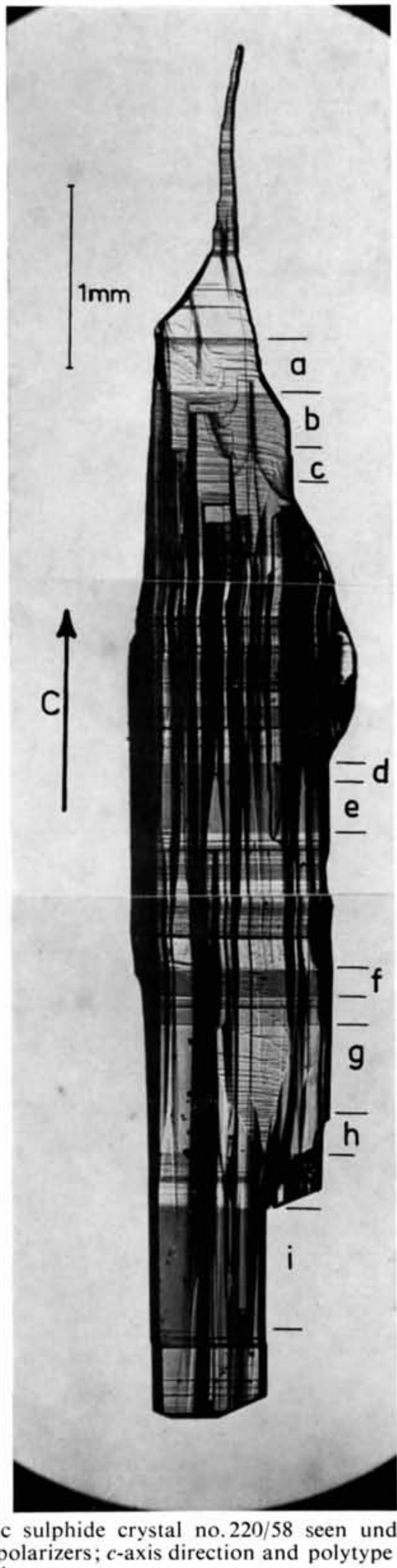

Fig. 1. Zinc sulphide crystal no. 220/58 seen under partially crossed polarizers; *c*-axis direction and polytype regions are indicated.

[To face p. 259

Table 5. *Comparison of observed and calculated intensities for the polytype* 72*R* (6 11 5 2)$_3$

l	Calc.	Obs.	l	Calc.	Obs.	Further observed relations between intensities
1	657	*w*	$\bar{2}$	457	*vw*	$\overline{23}>22$
4	799	*w*	$\bar{5}$	459	*vw*	$\overline{26}>\overline{20}\sim\overline{29}$
7	149	*vw*	$\bar{8}$	1386	*s*	$\overline{32}>\overline{14}>\bar{8}$
10	142	*vw*	$\overline{11}$	667	*w*	$25>34$
13	689	*w*	$\overline{14}$	2110	*s*	$\bar{2}\sim\bar{5}>7\sim10$
16	26	*a*	$\overline{17}$	755	*w*	
19	10565	*vs*	$\overline{20}$	5365	*vs*	
22	19815	*vvs*	$\overline{23}$	28120	*vvs*	
25	1140	*w*	$\overline{26}$	15056	*vs*	
28	9730	*vs*	$\overline{29}$	4896	*vs*	
31	9807	*vs*	$\overline{32}$	3106	*s*	
34	526	*w*	$\overline{35}$	298	*vw*	
37	261	*vw*	$\overline{38}$	403	*vw*	

Table 6. *Comparison of observed and calculated intensities for the polytype* 24*L* (7 10 5 2)

l	Calc.	Obs.	l	Calc.	Obs.	Further observed relations between intensities
0	1185	*vw*				
1	741	*vw*	$\bar{1}$	405	*vvw*	$7\sim8>9$
2	166	*vvw*	$\bar{2}$	308	*vvw*	$\bar{7}>7$
3	1128	*vw*	$\bar{3}$	662	*vw*	$\overline{10}>\bar{8}$
4	3159	*s*	$\bar{4}$	0	*a*	$\bar{9}>\bar{6}>4$
5	58	*vvw*	$\bar{5}$	1104	*vw*	$11>10$
6	242	*vvw*	$\bar{6}$	3371	*s*	$0\sim3>12>1$
7	18950	*vvs*	$\bar{7}$	27526	*vvs*	$\bar{5}>\overline{11}\sim\overline{12}>\bar{3}$
8	20177	*vvs*	$\bar{8}$	9368	*vs*	$6>2>5$
9	16448	*vvs*	$\bar{9}$	7530	*s*	$\bar{1}>\bar{2}$
10	1980	*w*	$\overline{10}$	14782	*vs*	
11	2563	*w*	$\overline{11}$	1317	*vw*	
12	1089	*vw*	$\overline{12}$	1089	*vw*	

Table 7. *Comparison of observed and calculated intensities for the polytype* 24*L* (16 4 2 2)

l	Calc.	Obs.	l	Calc.	Obs.	Further observed relations between intensities
0	1185	*w*				
1	1569	*w*	$\bar{1}$	273	*vvw*	$8>7>9$
2	617	*vw*	$\bar{2}$	617	*vw*	$\bar{7}>\bar{6}$
3	51	*vvw*	$\bar{3}$	710	*vw*	$12>1>0$
4	0	*a*	$\bar{4}$	0	*a*	$12>\bar{5}$
5	854	*vw*	$\bar{5}$	1937	*w*	$5>2$
6	6322	*vs*	$\bar{6}$	6322	*vs*	$\bar{9}>\bar{3}>\bar{2}$
7	15877	*vvs*	$\bar{7}$	7000	*vs*	
8	54767	*vvs*	$\bar{8}$	2882	*w*	
9	13588	*vvs*	$\bar{9}$	975	*vw*	
10	3961	*s*	$\overline{10}$	3961	*s*	
11	1019	*vw*	$\overline{11}$	5838	*vs*	
12	3267	*w*	$\overline{12}$	3267	*w*	

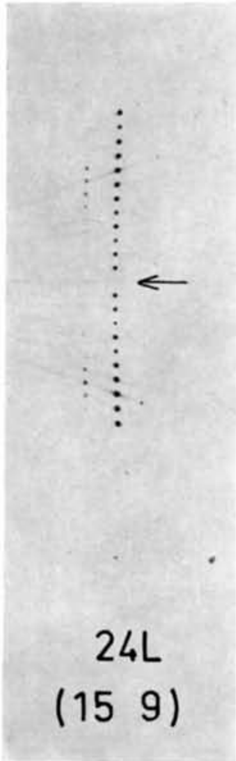

Fig. 2

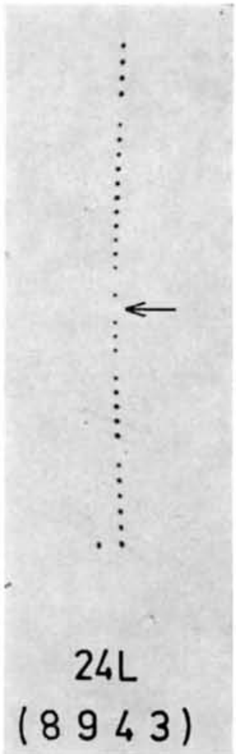

Fig. 3

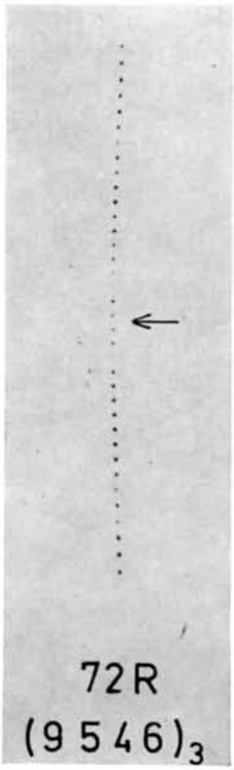

Fig. 4

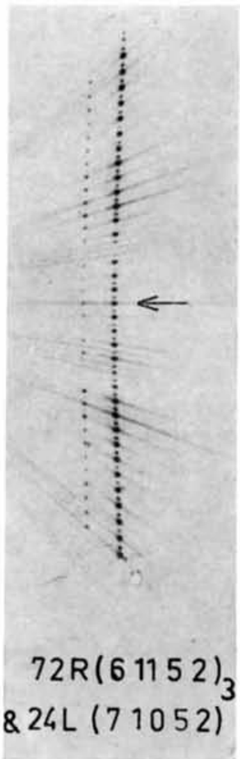

Fig. 5

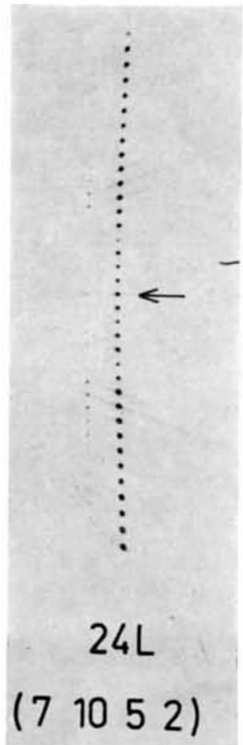

Fig. 6

Figs. 2–6. (10.*l*) column of oscillation photographs (× 3) about the *c* axis of the polytypes indicated. Cu $K\alpha$ radiation, 60 mm dia. camera. The position of the zero line is indicated by an arrow.

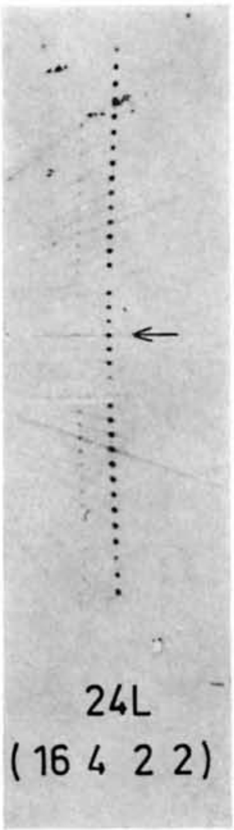

Fig. 7

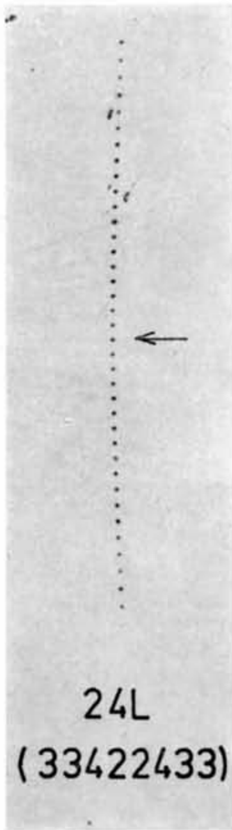

Fig. 8

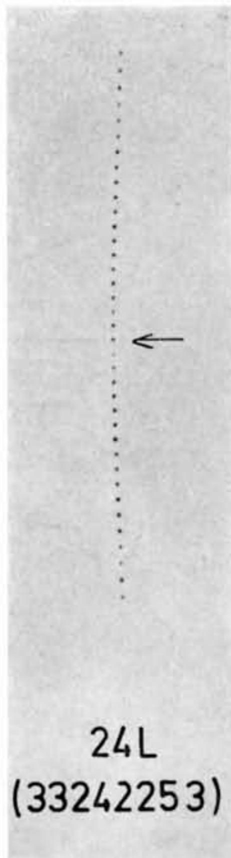

Fig. 9

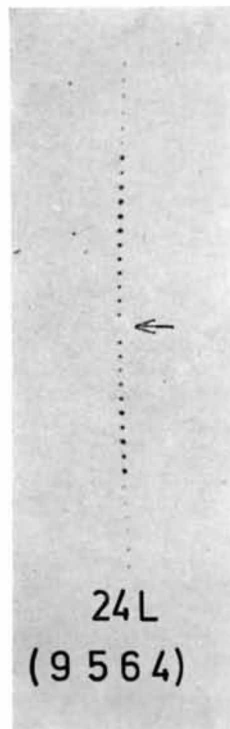

Fig. 10

Figs. 7–10. (10.*l*) column of oscillation photographs ($\times$ 3) about the *c* axis of the polytypes indicated. Cu $K\alpha$ radiation, 60 mm dia. camera. The position of the zero line is indicated by an arrow.

Table 8. *Comparison of observed and calculated intensities for the polytype* 24*L* (3 3 4 2 2 4 3 3)

l	Calc.	Obs.*	Further observed relations between intensities
0	1185	*vw*	8 > 12
1	847	*vw*	10 > 9 > 3
2	617	*vw*	0 > 1 > 2
3	1759	*w*	
4	4212	*s*	
5	6274	*vs*	
6	6322	*vs*	
7	4578	*s*	
8	20177	*vvs*	
9	2757	*w*	
10	3961	*w*	
11	4987	*s*	
12	13430	*vvs*	

* The observed intensities are symmetrical with respect to the zero line.

Of special interest are regions *d* and *e*. They are neighbouring regions and a very fine striation can be seen between them; region *d* is somewhat tilted with respect to region *e*. Region *e* is a 24 *L*(7 10 5 2) polytype and *d* is 72*R* (6 11 5 $2)_3$. It seems that region *d* is related to region *e* by a periodic slip process (Mardix, Alexander, Brafman & Steinberger, 1967) with a period of 24 layers and acting on the 7th layer. The calculated tilt angle for such a process is 1°41′ while the measured one was 1°30′ ± 20′.

Region *d* was too narrow to be photographed alone with a 0·1 mm collimator, so an oscillation photograph was taken of region *e* by itself (Fig. 6) and another one of regions *e* and *d* together (Fig. 5). The fact that these two regions are of the same family, only one of them being rhombohedral, enables the two polytypes to be clearly identified. An interesting fact is that no **c**-direction spikes can be seen on the common photograph; this indicates that any disordered transition region between these two polytypes, if it exists at all, must be very narrow.

References

Farkas-Jahnke, M. (1965). *Acta Cryst.* **18**, 571.

Mardix, S., Brafman, O. & Steinberger, I. T. (1967). *Acta Cryst.* **22**, 805.

Mardix, S., Alexander, E., Brafman, O. & Steinberger, I. T. (1967). *Acta Cryst.* **22**, 808.

Table 9. *Comparison of observed and calculated intensities for the polytype* 24*L* (3 3 2 4 2 2 5 3)

l	Calc.	Obs.	*l*	Calc.	Obs.	Further observed relations between intensities
0	1185	*vw*				
1	179	*vvw*	$\bar{1}$	2422	*w*	$7 > \bar{8} > 11$
2	617	*vw*	$\bar{2}$	617	*vw*	$4 \sim 12 > 10$
3	1759	*w*	$\bar{3}$	1759	*w*	$\bar{9} > \bar{1} > \bar{3}$
4	4212	*s*	$\bar{4}$	4212	*s*	$0 > 2 \sim \bar{2}$
5	2306	*w*	$\bar{5}$	4182	*s*	
6	6322	*vs*	$\bar{6}$	6322	*vs*	
7	21725	*vvs*	$\bar{7}$	6351	*vs*	
8	2882	*w*	$\bar{8}$	20177	*vvs*	
9	2757	*w*	$\bar{9}$	2757	*w*	
10	3961	*s*	$\overline{10}$	3961	*s*	
11	15829	*vvs*	$\overline{11}$	7482	*vs*	
12	4718	*s*	$\overline{12}$	4718	*s*	

Table 10. *Comparison of observed and calculated intensities for the polytype* 24*L* (9 5 6 4)

l	Calc.	Obs.	*l*	Calc.	Obs.	Further observed relations between intensities
0	0	*a*				
1	1176	*w*	$\bar{1}$	1015	*w*	$\bar{9} > \bar{7} > 8 > \bar{8}$
2	308	*vw*	$\bar{2}$	670	*w*	$10 > 6$
3	166	*vw*	$\bar{3}$	438	*vw*	$5 > 4 \sim 1$
4	1053	*w*	$\bar{4}$	1053	*w*	$11 > 12 > 9$
5	1959	*w*	$\bar{5}$	983	*w*	$\overline{10} > \overline{12}$
6	10354	*vs*	$\bar{6}$	4097	*s*	$\bar{1} > \bar{2}$
7	814	*w*	$\bar{7}$	25952	*vvs*	$2 > 3$
8	19456	*vvs*	$\bar{8}$	15133	*vvs*	
9	847	*w*	$\bar{9}$	31296	*vvs*	
10	11350	*vs*	$\overline{10}$	1980	*w*	
11	2336	*w*	$\overline{11}$	443	*vw*	
12	1452	*w*	$\overline{12}$	1452	*w*	